NASA TECHNICAL MEMORANDUM

NASA TM X-53126

SEPTEMBER 4, 1964

NASA TM X-53126

PERFORMANCE AND STABILITY OF ROCKET ENGINE INJECTORS USING LOX/RP-1 PROPELLANTS

by CURTIS R. BAILEY
Propulsion and Vehicle Engineering Laboratory

NASA

George C. Marshall Space Flight Center, Huntsville, Alabama

TECHNICAL MEMORANDUM X-53126

PERFORMANCE AND STABILITY OF ROCKET ENGINE INJECTORS USING LOX/RP-1 PROPELLANTS

By

Curtis R. Bailey
George C. Marshall Space Flight Center
Huntsville, Alabama

ABSTRACT

The performance and stability characteristics were determined for concentric tube (coaxial), micro-orifice, and impinging jet rocket engine injectors using LOX/RP-1 Propellants.

The concentric tube (fuel surrounding oxidizer) injector produced unstable combustion at all mixture ratios greater than 1.5; performance was high. Combustion was stable at all mixture ratios less than 1.5 and performance was lowered. The concentric tube (oxidizer surrounding fuel) injector was unsatisfactory. Although the micro-orifice injector produced stable combustion and moderately high performance, structural limitations of the micro-orifice material preclude its use. Performance of the impinging jet injector was marginal and combustion was stable.

Author

ENGINE SYSTEMS BRANCH
PROPULSION DIVISION

NASA-GEORGE C. MARSHALL SPACE FLIGHT CENTER

NASA - GEORGE C. MARSHALL SPACE FLIGHT CENTER

TECHNICAL MEMORANDUM X-53126

PERFORMANCE AND STABILITY OF ROCKET ENGINE INJECTORS USING LOX/RP-1 PROPELLANTS

By

Curtis R. Bailey

ENGINE SYSTEMS BRANCH
PROPULSION DIVISION
PROPULSION AND VEHICLE ENGINEERING LABORATORY
RESEARCH AND DEVELOPMENT OPERATIONS

TABLE OF CONTENTS

LIST OF ILLUSTRATIONS

LIST OF ILLUSTRATIONS (Concluded)

LIST OF TABLES

DEFINITION OF SYMBOLS

A_t	Nozzle Throat Area
C*	Characteristic Velocity
F	Thrust
g	Acceleration Due to Gravity
L*	Characteristic Chamber Length
Pc	Combustion Chamber Pressure
ΔPf	Differential Fuel Injection Pressure
ΔPo	Differential Oxidizer Injection Pressure
MR	Propellant Mixture Ratio, Oxidizer/Fuel
Wf	Fuel Flowrate
Wo	Oxidizer Flowrate
ηc^*	Characteristic Velocity Efficiency, Based on Shifting Equilibrium

CONVERSION FACTORS

Pound force = 4.4482 newton

Pound force/inch^2 = 6890 newton/meter^2

Pound mass = .4536 kilogram

Inch = 2.54 X 10^{-2} meter

Gallon (U.S. Liq.) = 3785.4 X 10^{-6} meter^3

Feet/second = .3048 meter/second

TECHNICAL MEMORANDUM X-53126

PERFORMANCE AND STABILITY OF ROCKET ENGINE INJECTORS USING LOX/RP-1 PROPELLANTS

SUMMARY

The performance and stability characteristics were determined for several types of rocket engine injectors using liquid oxygen and RP-1 as propellants. The injector types tested were concentric tube (coaxial), micro-orifice, and impinging jet. The concentric tube injector was tested with the propellants injected in the usual manner (fuel surrounding oxidizer) and with the oxidizer surrounding the fuel.

Nominal thrust chamber pressure was 6.89 MN/m^2 (1000 psia), producing a thrust of approximately 17800 newtons (4000 pounds). Propellant mixture ratios varied from .50 to 3.0.

The concentric tube (fuel surrounding oxidizer) injector produced unstable combustion at all mixture ratios greater than 1.5. Performance was high. Combustion was stable and performance was lowered with mixture ratios lower than 1.5. Attempts to drive the combustion unstable by pneumatically pulsing the fuel feed line were unsuccessful.

The concentric tube (oxidizer surrounding fuel) injector proved unsatisfactory. Performance was moderate, the combustion was unstable, and injector face heating was severe.

The micro-orifice injector produced stable combustion with moderate performance. However, micro-orifice material did not prove suitable for injector face applications because of structural limitations.

Performance of the impinging jet injector was marginal; however, this conclusion is based on very limited testing. No instability was measured except for chugging during the shutdown of one firing.

Chamber pressure transducers mounted flush with the combustion chamber wall were unable to withstand the heating rates during periods of unstable combustion. Protective transducer adaptors alleviated the heating problem but created resonant frequencies which hampered

measurement of the frequencies within the combustion chamber.

Continued effort is recommended to investigate the causes of combustion instability created by the concentric tube injector. Use of the unstable injector as a test tool to evaluate experimental pressure transducers is also recommended.

INTRODUCTION

Successful development of a modern rocket engine system depends, to a large extent, upon the adequacy of its propellant injection system. High performance and stable combustion are the usual criteria of rocket engine design, and both, to a very high degree, are functions of injector design. Today, injector design remains somewhat of an art, for the performance and stability characteristics of a particular configuration can seldom be predicted accurately. Test programs are, therefore, required for the evaluation of each injector type, or configuration, that appears promising. These programs are conducted at relatively low thrust levels to quickly and economically eliminate unsatisfactory designs.

This investigation was conducted to determine and compare the performance and stability characteristics of several types of rocket motor injectors using LOX and RP-1 as propellants. The results of the engine test program are presented with recommendations for further investigation of the causes of combustion instability in LOX/RP-1 combustion chambers.

The author acknowledges the help of members of Components Test Laboratory A and the Vibration Data System Section, George C. Marshall Space Flight Center, in conducting this program. Special thanks also goes to Mr. Preston Layton, Princeton University, for his aid with transient pressure measurement problems and subsequent data interpretation.

THRUST CHAMBER AND INJECTOR CONFIGURATIONS

The rocket engine used in all firings had an uncooled copper combustion chamber and a water-cooled nozzle. The chamber was equipped with a removable 7.6 cm (3.0 in) section so that characteristic length (L*) could be varied between runs. The assembly is shown in

FIG 1. Nominal thrust rating of the chamber at 6.89/ MN/m^2 (1000 psia) chamber pressure was 17800 newtons (4000 pounds).

The chamber diameter was 9.48 cm (3.73 in) and the nozzle throat diameter was 4.45 cm (1.75 in), with a corresponding contraction ratio of 4.5. Characteristic length (L*) was 1.205 meters (47.5 in) with the 7.6 cm (3.0 in) chamber section installed and 86.4 cm (34.0 in) with the section removed. An uncooled nozzle extension having an exit diameter of 17.8 cm (7.0 in) was provided giving an area ratio of 16.0.

Fuel resistant rubber O-rings were used throughout the engine assembly except for the asbestos gaskets used in the 7.6 cm (3.0 in) chamber insert and a metal O-ring that served as the hot gas seal between the chamber and injector.

The injector designs tested are shown in FIG 2 through 4. The concentric tube injector, shown in FIG 2, was tested both with fuel surrounding oxidizer and with oxidizer surrounding fuel. The design used 152 stainless steel tubes welded to the stainless steel injector body using either the electron beam or TIG (tungsten-inert gas) welding process.

For all firings with fuel surrounding oxidizer, a stainless steel injector face was used. Face thickness was initially .396 cm (.156 in), but overheating was encountered and the thickness was reduced to .320 cm (.126 in), eliminating the face heating problem. However, the stainless steel face was inadequate for the heating rates in the oxidizer-surrounding-fuel configuration, and a .534 cm (.210 in) thick copper face was used.

The micro-orifice injector shown in FIG 3 used alternating fuel and oxidizer rings with a face of micro-orifice material. The micro-orifice material was a .025 cm (.010 in) sheet of nickel alloy having a three percent open area of .0127 cm (.005 in) diameter holes. The face, formed by stamping, was welded to the stainless steel body with an electron beam welder.

The impinging jet injector shown in FIG 4 is similar to those used in several production LOX/RP-1 engines. Fabrication of the injector was similar to that of the micro-orifice configuration; electron beam welding was used to attach the face to the injector body. The face and body are of stainless steel.

TEST INSTALLATION AND OPERATION

The test installation used for all firings was located at Components Test Laboratory A, George C. Marshall Space Flight Center, and is pictured in FIG 5. A schematic of the cooling water and propellant systems is shown in FIG 6.

Propellants were supplied from 1.89 cubic meter (500 gal.) tanks that were pressurized with gaseous nitrogen. Triethylalumium (TEA), pressurized by the fuel system, was used as the ignition source. Nominal TEA flowrate was .091 kg/sec (.2 lb/sec). The main propellant valves were Hydromatic ball valves, and the TEA valve was an Annin poppet valve. These valves were controlled by Marotta solenoid valves. Sequencing of the propellant and TEA valves was accomplished either by orificing the pneumatic lines or by electrical sequencing of the control valves.

The engines were started by opening the TEA, oxidizer, and fuel valves in sequence, subsequent to chilling the oxidizer supply line with a LOX bleed. An oscillograph trace of a typical starting sequence is shown in FIG 7. Automatic cutoff was initiated if chamber pressure was not at least 1.89 MN/m^2 (275 psi) within one and one-half seconds after firing command. Since a heat-sink type combustion chamber was used, test duration was limited to not more than five seconds. The engine was shut down by closing the main propellant valves which were sequenced to provide a fuel-rich cutoff.

A pneumatically operated pulse inducer was installed in the fuel feed line immediately upstream of the injector, and was used in attempts to drive the combustion unstable. The design and operation of the pulse inducer is described in "Experimental Evaluation of the Pneumatic Operated Pulse Inducer", Report No. 1066, dated May 9, 1962, Chrysler Corporation Missile Division.

INSTRUMENTATION AND DATA REDUCTION

Instrumentation was provided for the measurement of thrust, oxidizer and fuel flowrates, oxidizer and fuel injection pressures, and both steady state and transient chamber pressure.

Thrust measurements were made with a Baldwin load cell that restrained the movement of a suspended thrust stand. The load cell was calibrated by applying loads through a calibrated proving ring and measuring deflection of the ring. Overall accuracy of the thrust measurements were within ± 3.0 percent.

Propellant flow measurements were made with water-calibrated Potter turbine flowmeters that provided a volumetric flow measurement. Mass flowrate was then obtained by multiplying volume flowrate by propellant density. Oxidizer density was determined from a temperature measurement taken by a chromel-alumel thermocouple placed upstream of the flowmeter. Overall accuracy of the flow measurements were within ± 2.0 percent.

Propellant injection pressure measurements were made initially with Wianko variable reluctance transducers, but frequency response was limited to approximately 600 cycles/sec. Dynisco strain gage transducers were later installed, raising the response of the system to approximately 4000 cycles/sec. These transducers were calibrated using a dead-weight tester, and measurement accuracy was within ± 1.5 percent.

Steady state chamber pressure was measured with either a Wianko variable reluctance or CEC (Consolidated Electrodynamics Corporation) strain gage transducer. The transducer was connected to the chamber with a short length of tubing. The frequency response was approximately 200 cycles/sec; overall accuracy was within ± 1.5 percent. A dead-weight tester was used for calibration.

Transient chamber pressure measurements were made using Dynisco models PT-130 and PT-49 and Photocon model 352A pressure transducers. These transducers are water cooled and are supposed to be mounted flush with the chamber wall for maximum frequency response. However, the heating rate was excessive during periods of unstable combustion, and it was necessary to install the transducers in protective adaptors. The adaptor is shown in FIG 1. Use of the adaptor protected the transducers but drastically reduced the frequency response of 10,000 cycles/sec when flush mounted. From calibration tests using helium and nitrogen, it has been estimated that with combustion products the transducer with adaptor has an amplitude response ratio of 2.5 at 1800 cycles/sec and .3 at 7000 cycles/sec.

Initially, all data except transient chamber pressure were recorded on Leeds and Northrup strip chart recorders and CEC oscillographs. Later, a System Engineering Laboratories digital instrumentation system was used. High frequency chamber pressure data were stored by an Ampex FR 600 tape recorder and later transferred to a CEC oscillograph. Both the oscillograph and tape recorder were operated at speeds up to 152 cm/sec (60 in/sec). The data stored on the tape were then digitized with an analog-to-digital convertor at a sampling rate of 20,000 samples per second.

After digitization, the data were analyzed using an IBM 7094 random vibration analysis program. For most applications the data were processed with a ten cycles per second filter over a total bandwidth of 10,000 cycles per second. Reduced data were then presented by an automatic digital plotter in the form of rms pressure as a function of frequency.

The rocket engine performance was based on calculation values of characteristic velocity (C*). Characteristic velocity is computed as follows:

$$C^* = \frac{P_c A_t g}{W}$$

Where: C^* = Characteristic Velocity

P_c = Chamber pressure

A_t = Nozzle throat area

g = Gravitational acceleration

W = Propellant flowrate

The chamber pressure term that appears in this equation is the isentropic stagnation pressure at the throat of the nozzle. The pressure measurements used for characteristic velocity calculations were the chamber static pressure measurements taken near the injector. The ratio of these two pressures approaches 1.0 as nozzle contraction ratio is increased. Since the contraction ratio of the nozzle used was large (4.55), the two pressures were assumed to be equal.

DISCUSSION OF TEST RESULTS

Concentric Tube Injector (Fuel Surrounding Oxidizer)

The concentric tube injector was originally designed so that the ends of the oxidizer tubes were flush with the injector face. Because of loose tolerances, the first injector fabricated had oxidizer tube ends that were recessed approximately .025 cm (.010 in) within the face. The design flow coefficients of .70 were verified during cold flow calibrations. However, during the first two firings, flow coefficients were severely reduced. Since injector face heating had also been a problem during these firings, the face thickness was reduced .076 cm (.030 in) allowing the oxidizer tubes to extend past the face approximately .051 cm (.020 in). This modification eliminated the face heating problem and also substantially raised the flow coefficients. Flow data is presented in FIG 8; note that the average values of the coefficients for runs 3 through 7 are significantly higher than for runs 1 and 2. The sudden expansion of the oxidizer at the exit of the tubes, which were recessed slightly within the face, is believed to have caused restriction of both propellants.

Fourteen firings were conducted using this injector at mixture ratios between 1.5 and 3.2. As shown in FIG 9 and Table 1, performance was fairly high, particularly at mixture ratios of around 2.2. Two of the firings (runs 33 and 34) produced characteristic velocities that were substantially lower than normal. The data points for these firings at mixture ratios of 2.35 and 2.05 are shown on FIG 9. A check of the injector, which had not been fired prior to run no. 33, revealed that more than half of the fuel ports were drilled .0076 cm (.003 in) undersize. It was concluded that the combination of increased fuel injection velocity and staggered mixture ratio across the injection face caused a decrease in characteristic velocity of approximately 153 m/sec (500 ft/sec).

The combustion produced by this injector proved to be consistently unstable at mixture ratios greater than 1.5. The frequency analyses for run no. 25, which is considered to be a typical run, are shown in FIG 10 through 14. The analysis of the chugging mode, which started immediately after ignition, is shown in FIG 10. Note that the predominant frequency is 100 cps at an rms amplitude of .276 MN/m^2 (40 psi), and the secondary frequency is 7900 cps at an rms amplitude of .076 MN/m^2 (11 psi). After approximately one second of chugging, a high frequency instability was triggered and persisted for the remainder of the firing. This instability was monitored by three dynisco pressure transducers

positioned as shown in FIG 1. Transducers No. 2 and 4 were mounted in protective adaptors and transducer No. 3 was flush mounted in the chamber.

The frequency analysis of the data from transducer No. 3 is shown in FIG 11. FIG 12 shows the corresponding peak-to-peak amplitudes as presented by a digital plotter. The predominant frequency of 7300 cps at an rms amplitude of 1.51 MN/m^2 (220 psi) corresponds to the theoretical first tangential mode.

The frequency analysis data from transducers No. 2 and 4 are presented in FIG 13 and 14. FIG 13 demonstrates rather clearly why protective transducer adaptors are usually inadequate for use in stability measurements. The fundamental resonant frequency of the adaptor cavity appears at 1800 cps and the third and fifth harmonics are evident at 5500 cps and 9100 cps. The first tangential mode at 7300 cps shows an rms amplitude of only .461 MN/m^2 (67 psi) which, compared with the data in FIG 11, gives a response ratio of approximately 0.3. The data from transducer No. 4 (FIG 14) also include the adaptor resonances and tangential frequency. The peak at 2500 cps may be the fundamental longitudinal mode, but it cannot be positively identified since it is not predominant in either of the other analyses.

Nine test firings were conducted (at mixture ratios varying from .48 to 70), to determine if the concentric tube injector would yield higher combustion efficiencies than current LOX-RP-1 impinging jet gas generator designs. Runs No. 6 and No. 12 through 16 were conducted with a chamber L* of 1.22 m (48 in). Runs No. 20 through 22 used an L* of 0.86m (34 in). For these firings, LOX tube size was reduced to .079 cm (031 in) ID, .119 cm (.047 in) OD for all runs except No. 6 which utilized .109 cm (.043 in) ID, 160 cm (.063 in) OD tubes. Diameter of the fuel annulus was .193 cm (.076 in) for all firings.

Test results are tabulated in Table 1 and FIG 15. FIG 16 shows an extrapolation of the results of these firings to a chamber L* of 2.11m (83 in) corresponding to the effective L* of the F-1 gas generator. As shown on the plot, the extrapolated C* efficiency at this L* is 92%; this is somewhat higher than the experimental F-1 gas generator data point. Obviously, C* efficiency cannot increase indefinitely as L* increases, and a concentric tube injector test firing at an L* of 2.11m (83 in) might approximate the F-1 gas generator data point.

All firings at gas generator mixture ratios were stable except run no. 6. During run no. 6, severe chugging was observed; peak-to-peak amplitudes of 1.51 MN/m^2 (220 psi) at 100 cps were recorded. This was the only run using the large LOX tubes with corresponding low oxidizer differential injection pressure.

FIG 17 shows the amplitudes of the predominant frequencies recorded during run no. 21; this may be considered typical of the stable firings. Fuel feed line pulsing was employed in runs no. 21 and 22 to determine the stability characteristics of the configuration. An oscillogram trace showing the pulse pressures during run no. 21 is shown in FIG 18. It is apparent that the pressures generated by the low energy pulser were too low to be of much significance.

Concentric Tube Injector (Oxidizer Surrounding Fuel)

Three firings were conducted using the concentric tube injector with propellant injection reversed so that oxidizer surrounded each fuel stream. The stainless steel face injector was badly burned during the first firing (run no. 32). A new injector with a copper face was fabricated and tested in firings no. 45 and 46. Firing no. 45 was inadvertently terminated before mainstage was reached. The injector face overheated during firing no. 46, causing structural failure of the face plate centerpost.

Combustion instability occurred during the final firing but failure of pressure transducers prevented obtaining a record of sufficient duration to conduct a frequency analysis. It appeared that the instability was a combination of first tangential and first longitudinal modes with a resultant peak-to-peak amplitude of 5.51 MN/m^2 (800 psi). No further testing was conducted using this configuration, because it showed no improvement over the 'fuel surrounding oxidizer" injector in either performance or combustion stability and had, in addition, an inherent severe face heating problem.

Micro-Orifice Injector

As shown in FIG 3, TEA (Triethylaluminum) was to be injected through the center of the micro-orifice face. During the calibration flow checks, TEA flow through the micro-orifice material was inadequate. Several small holes were drilled through the face to increase the TEA injection area; this modification provided normal TEA flow.

Five firings were conducted using the micro-orifice injector. The first firing (run no. 18) was prematurely terminated by the low chamber pressure cutoff when a detonation in the chamber damaged the pressure transducer. The second firing (run no. 19) was satisfactory with C* efficiency of 90 percent and no damage to the injector. As shown in FIG 19, combustion was very stable with an rms amplitude of 052. MN/m^2 (7.5 psi) at 100 cps.

During the third firing (run no. 23) the chamber pressure transducer was again destroyed by a detonation in the chamber during thrust buildup. The injector was also destroyed; most of the micro-orifice material was torn from the weld. A new face was installed on the injector body and the configuration was tested in two additional firings. Run no. 35 was satisfactory - stable combustion and a C* efficiency of 86 percent. There was no damage. Another detonation during thrust buildup occurred in the second firing (run no. 36) of this injector. The chamber pressure transducer was destroyed, and the micro-orifice face was severely damaged.

The detonations are not believed to be the prime cause of failure of the injector faces. Apparently flexing of the face at the electron beam weld caused cracking and failure; the use of thicker micro-orifice material or different fabrication techniques might alleviate this problem. The cause of the detonations is believed to be poor TEA dispersion; axial injection of TEA created a TEA-oxidizer flame along the center line of the chamber during ignition. Localized ignition sources of this type have previously been unreliable in providing smooth starts.

Impinging Jet Injector

Three firings were conducted using the impinging jet injector. The injector face was severely burned during the first firing (run no. 17). The injector was repaired; the face thickness was reduced from .254 cm (.10 in) to .127 cm (.05 in) to eliminate face burning. This modified configuration was tested in runs no. 30 and 31. Burning of the face was substantially reduced, but overheating continued to be a major problem. FIG 20 shows the condition of the face after run no. 30. After another firing (run no. 31), the injector was unsuitable for further testing. Installation of a copper face might have eliminated the heating problem, but it was not known if electron beam welding was suitable for joining copper to stainless steel.

As shown in FIG 9, the performance of the impinging jet injector was marginal. No significant combustion instability was observed during the firings except for 150 cycle/sec chugging during shutdown of run no. 30. FIG 21 shows the pressure amplitudes of the predominant frequencies present during run no. 31.

CONCLUSIONS

As a result of this program, it is concluded that:

1. The concentric tube (fuel surrounding oxidizer) injector in the tested configuration produces unstable combustion with high level of performance (characteristic velocity) at normal thrust chamber propellant mixture ratios. At gas generator mixture ratios, combustion is stable, but performance is lower. If propellant injection is reversed (oxidizer surrounding fuel), performance is moderate, combustion is unstable, and injector face heating is a problem.

2. In the configuration tested, micro-orifice material does not appear to be a suitable face material for LOX-RP-1 injectors in rocket motors. With the micro-orifice injector, combustion is stable, but performance is moderate and the micro-orifice material cracks. No attempt was made to solve the problem of material failure by changing fabrication techniques.

3. The impinging jet injector is a common type and was selected as a standard for judging the other injectors tested. However, the performance of this particular configuration is marginal; combustion was stable except for chugging during shutdown of one firing.

4. Adaptors designed to protect chamber pressure transducers from the high heat flux encountered with flush mounted installations are usually inadequate. Adaptor cavity resonances prevent accurate measurement of the frequencies within the combustion chamber. The commercial pressure transducers tested were not able to withstand the heating rates encountered during periods of instability when flush-mounted in the combustion chamber.

RECOMMENDATIONS

Investigations should be conducted to determine the cause of instability in the concentric tube injector; the effects of propellant premixing cups and changes in burning rate should be studied.

The unstable injector and motor assembly should be used as a test instrument for evaluating other pressure transducers and transient pressure measurement techniques.

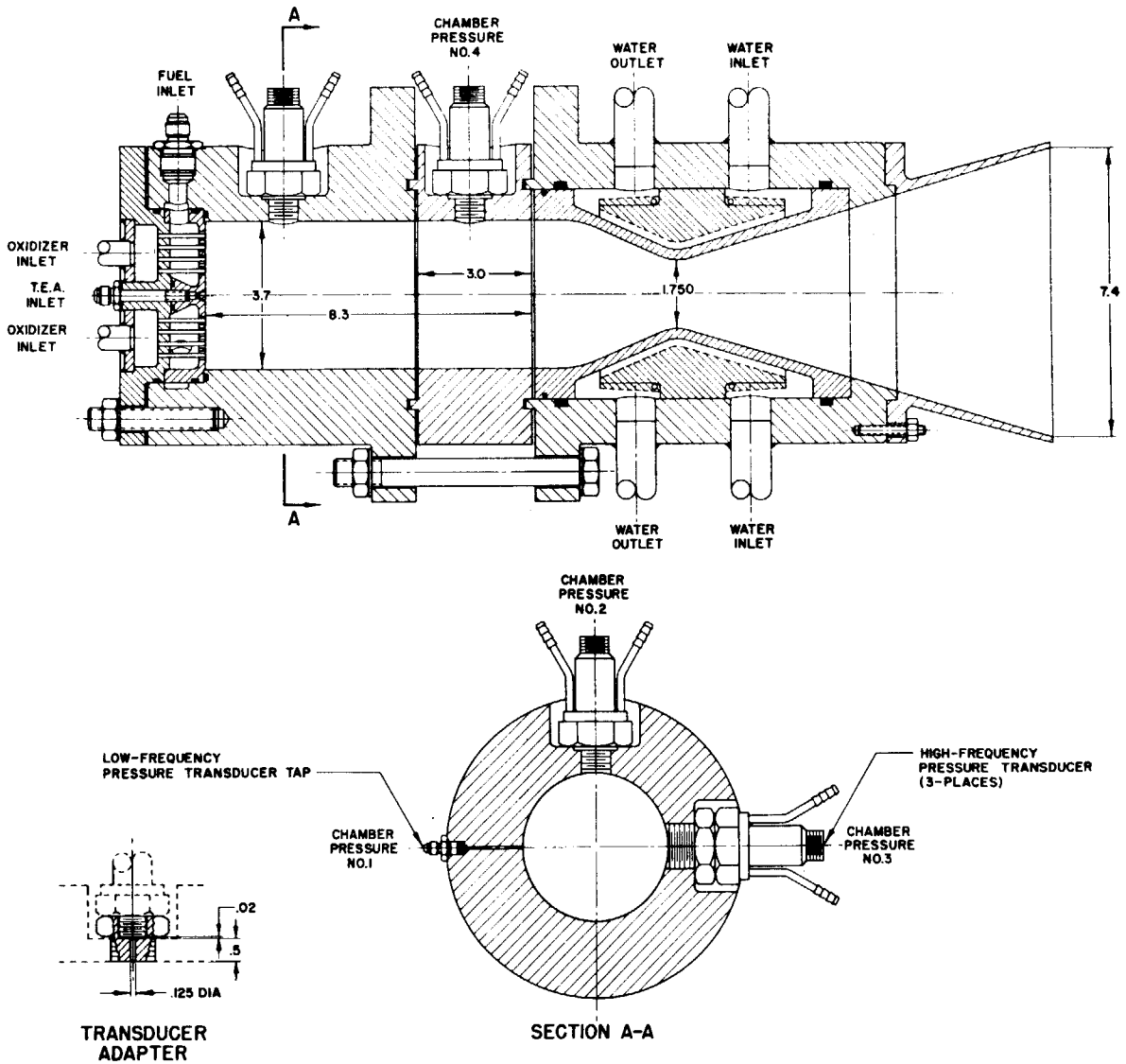

FIGURE 1
THRUST CHAMBER ASSEMBLY
(English System Dimensions)

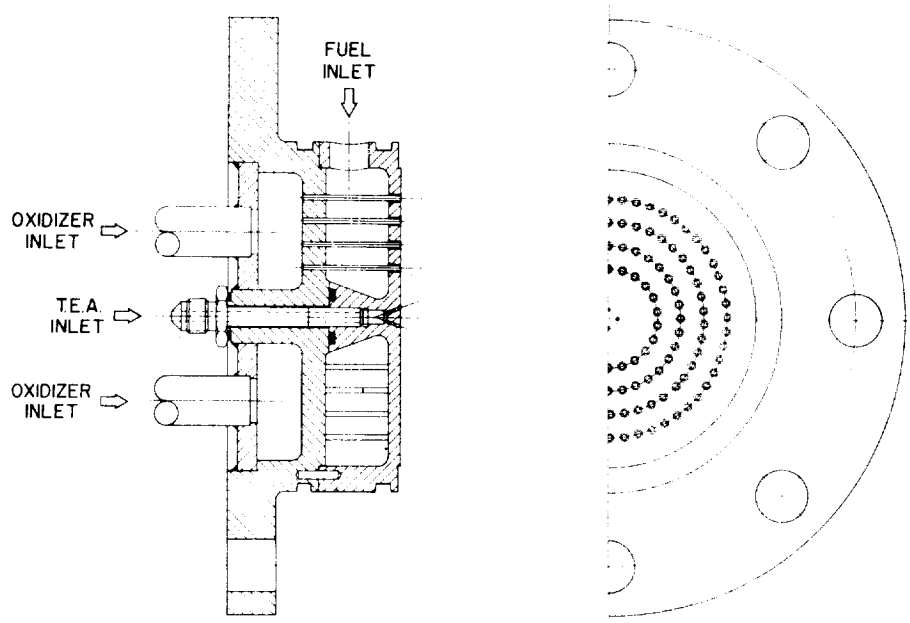

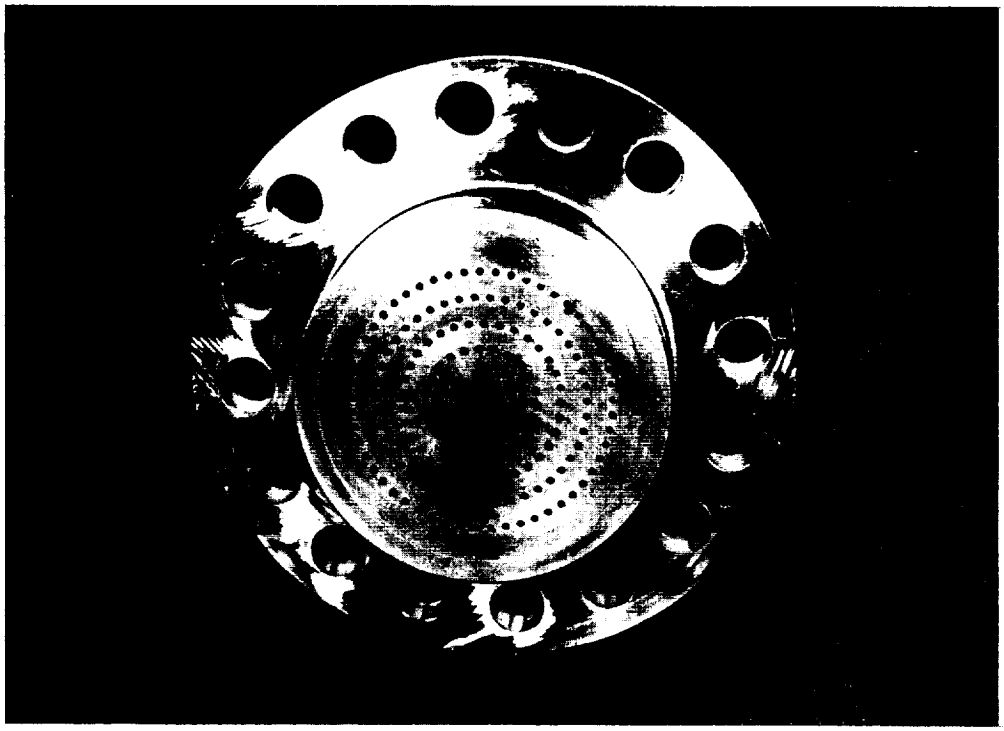

FIGURE 2. CONCENTRIC TUBE INJECTOR

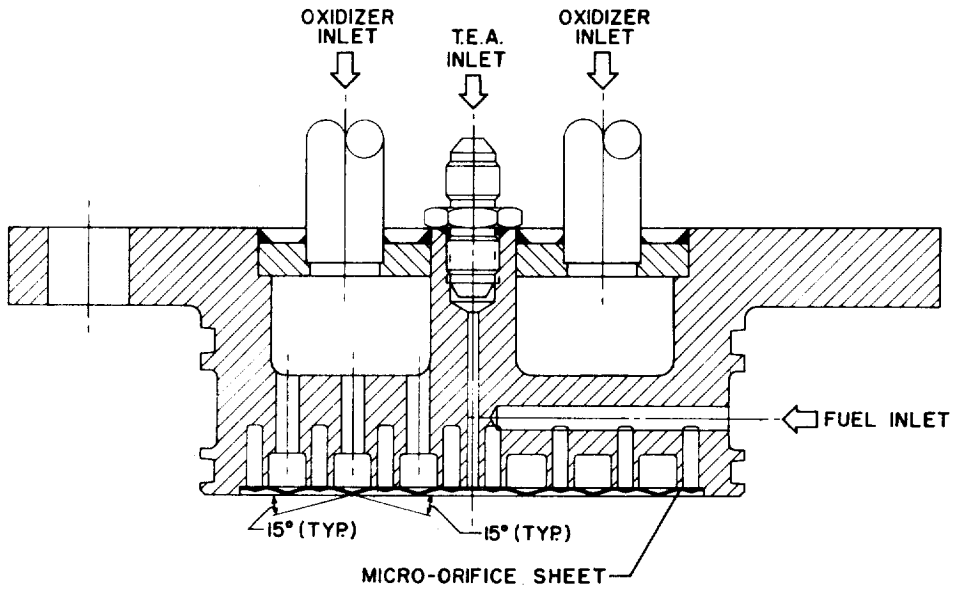

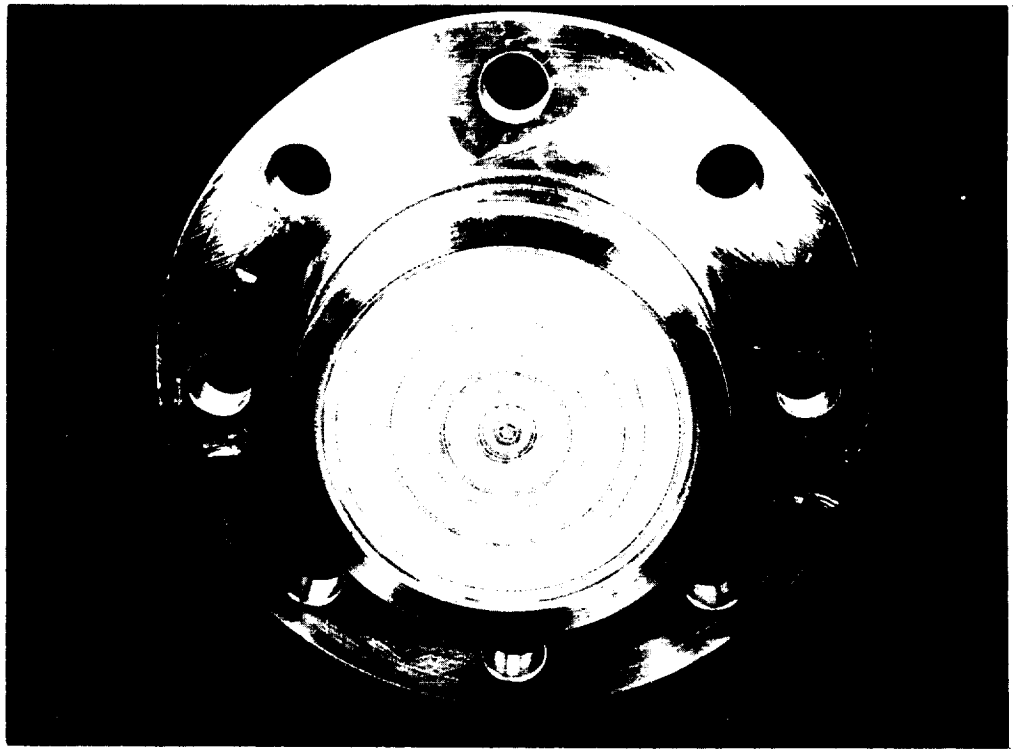

FIGURE 3. MICRO-ORIFICE INJECTOR

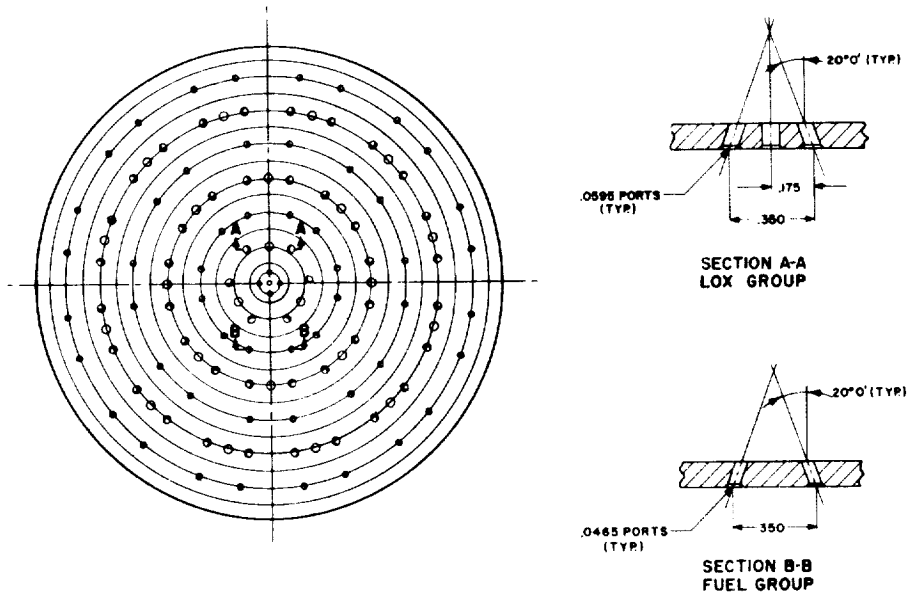

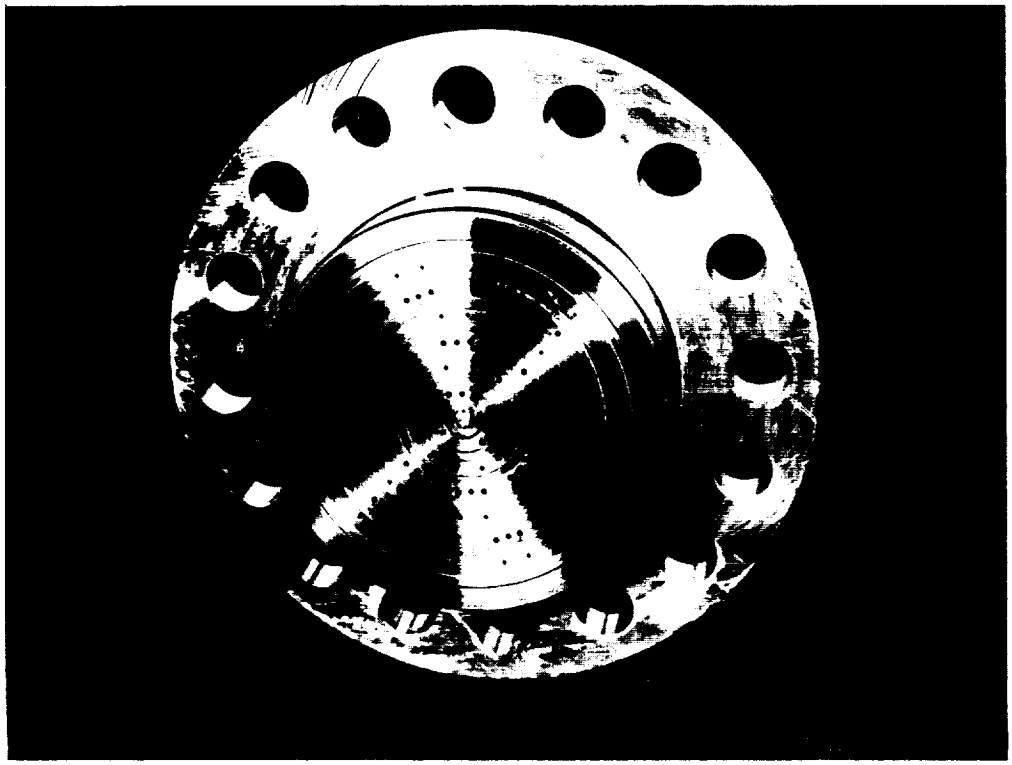

FIGURE 4. IMPINGING JET INJECTOR

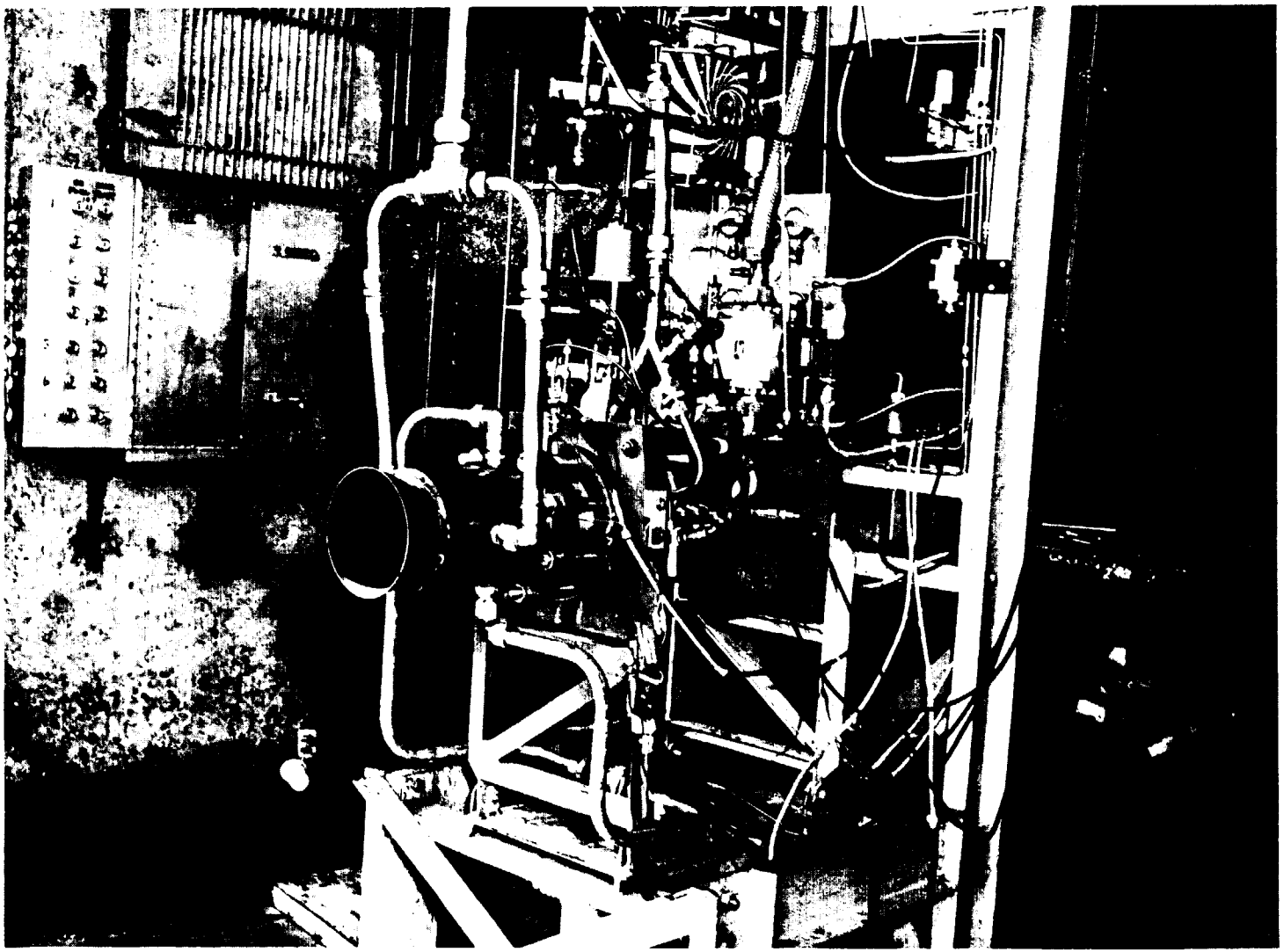

FIGURE 5. EXPERIMENTAL INJECTOR TEST INSTALLATION

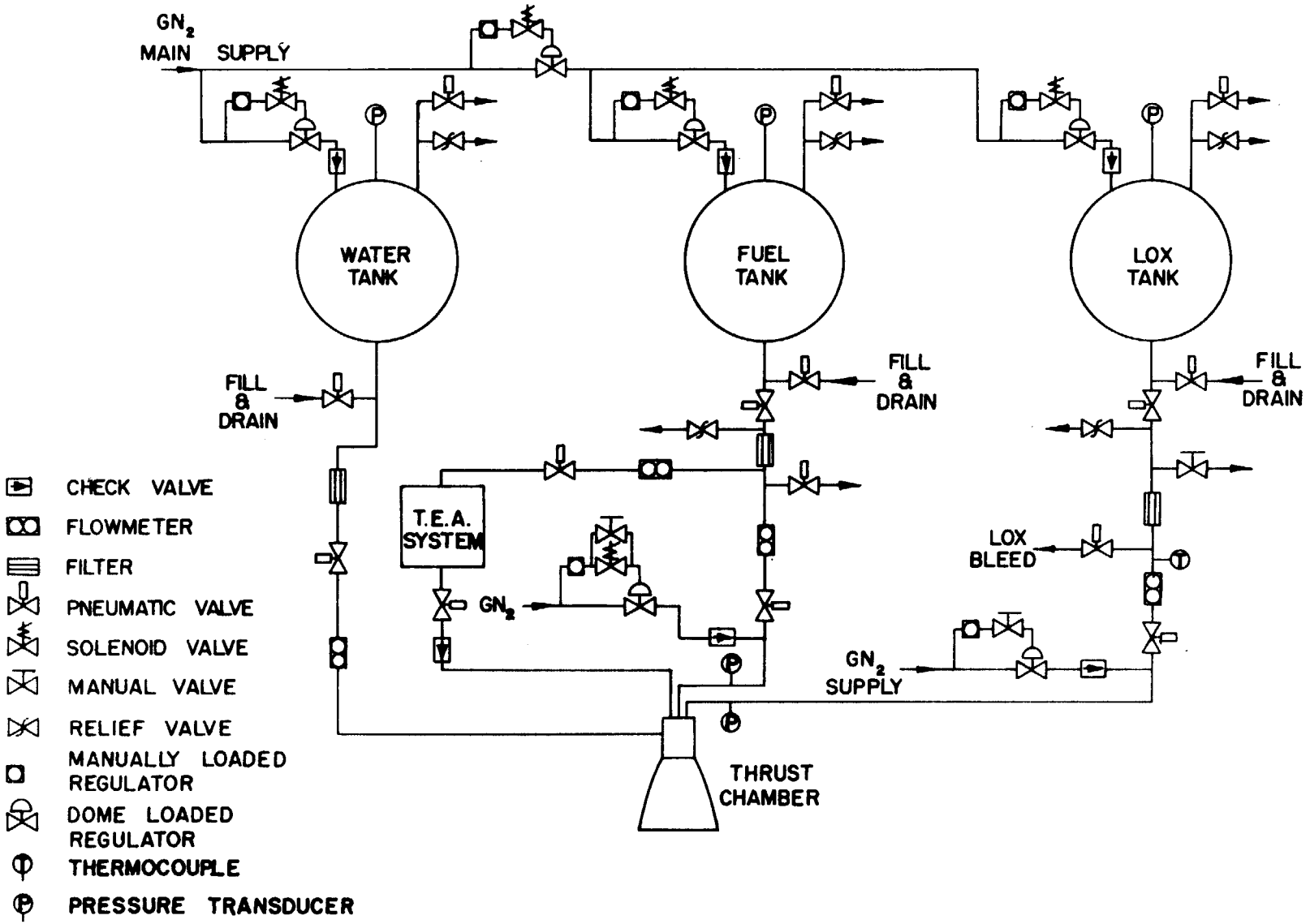

FIGURE 6. TEST INSTALLATION SCHEMATIC

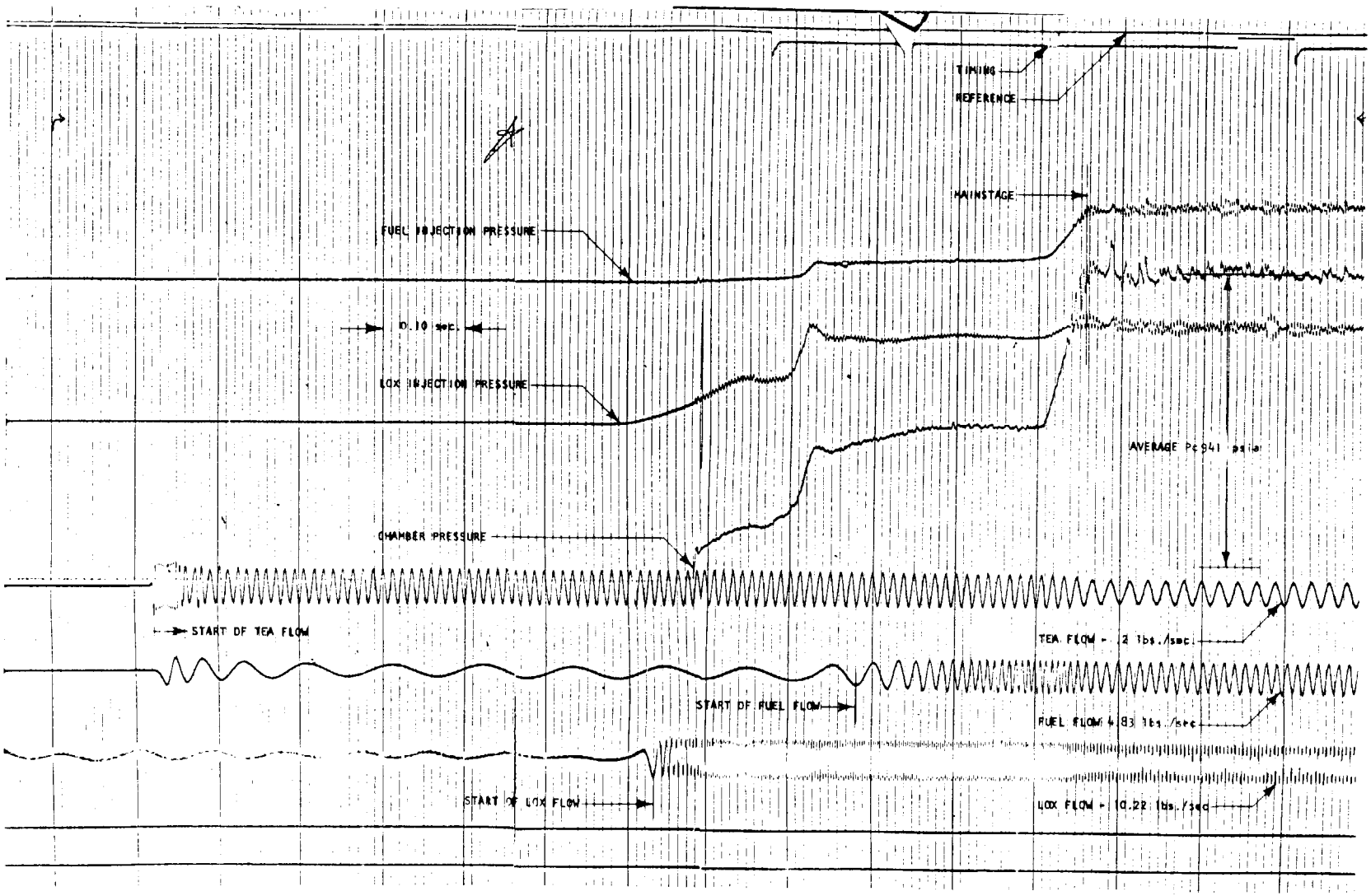

FIGURE 7. OSCILLOGRAM OF TYPICAL STARTING SEQUENCE

Run No.	Sketch No.	Injector Configuration			RP-1 Flow Coef.	RP-1 Reynolds No.	LOX Flow Coef.	LOX Reynolds No.
		Dim. A (in)	Dim. B (in)	Dim. C (in)				
1	1	.158	.070	.010	.386	1540	.515	190,000
2	1	.158	.073	.010	.353	2520	.425	167,000
3	2	.128	.076	.020	.672	2950	.718	200,000
4	2	.128	.076	.020	.576	2420	.659	232,000
5	2	.128	.076	.020	.640	2460	-	-
6	2	.128	.076	.020	.557	4080	.744	126,000
7	2	.128	.070	.020	.610	2700	.610	240,000

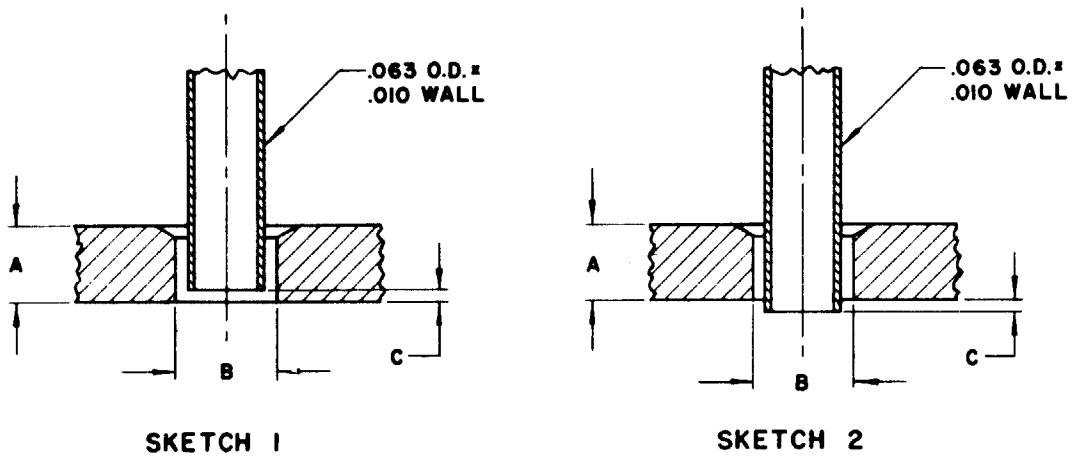

FIGURE 8. CONCENTRIC ORIFICE INJECTOR FLOW DATA

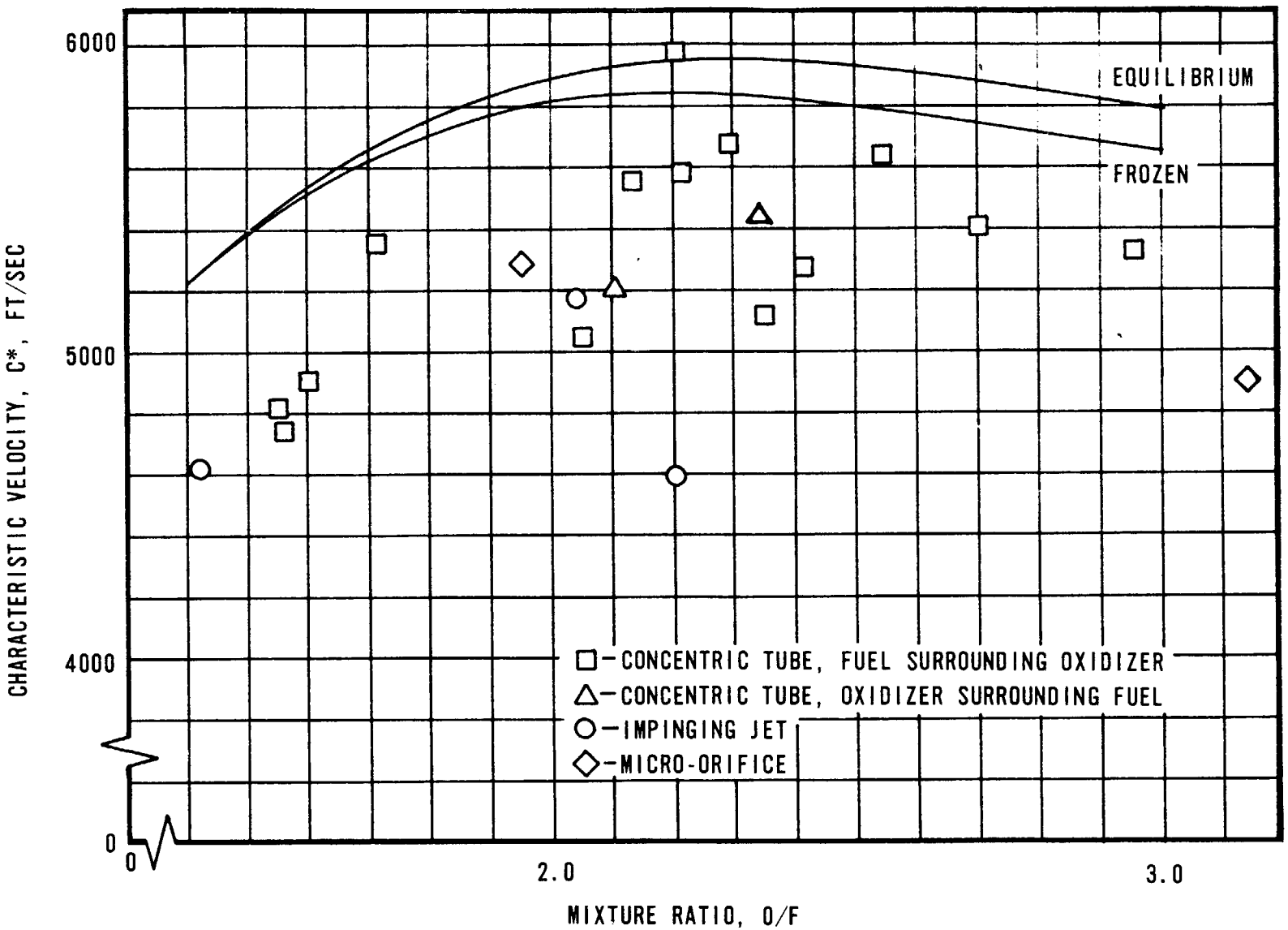

FIGURE 9. CHARACTERISTIC VELOCITY AS A FUNCTION OF MIXTURE RATIO, M.R. 1.4 - 3.2

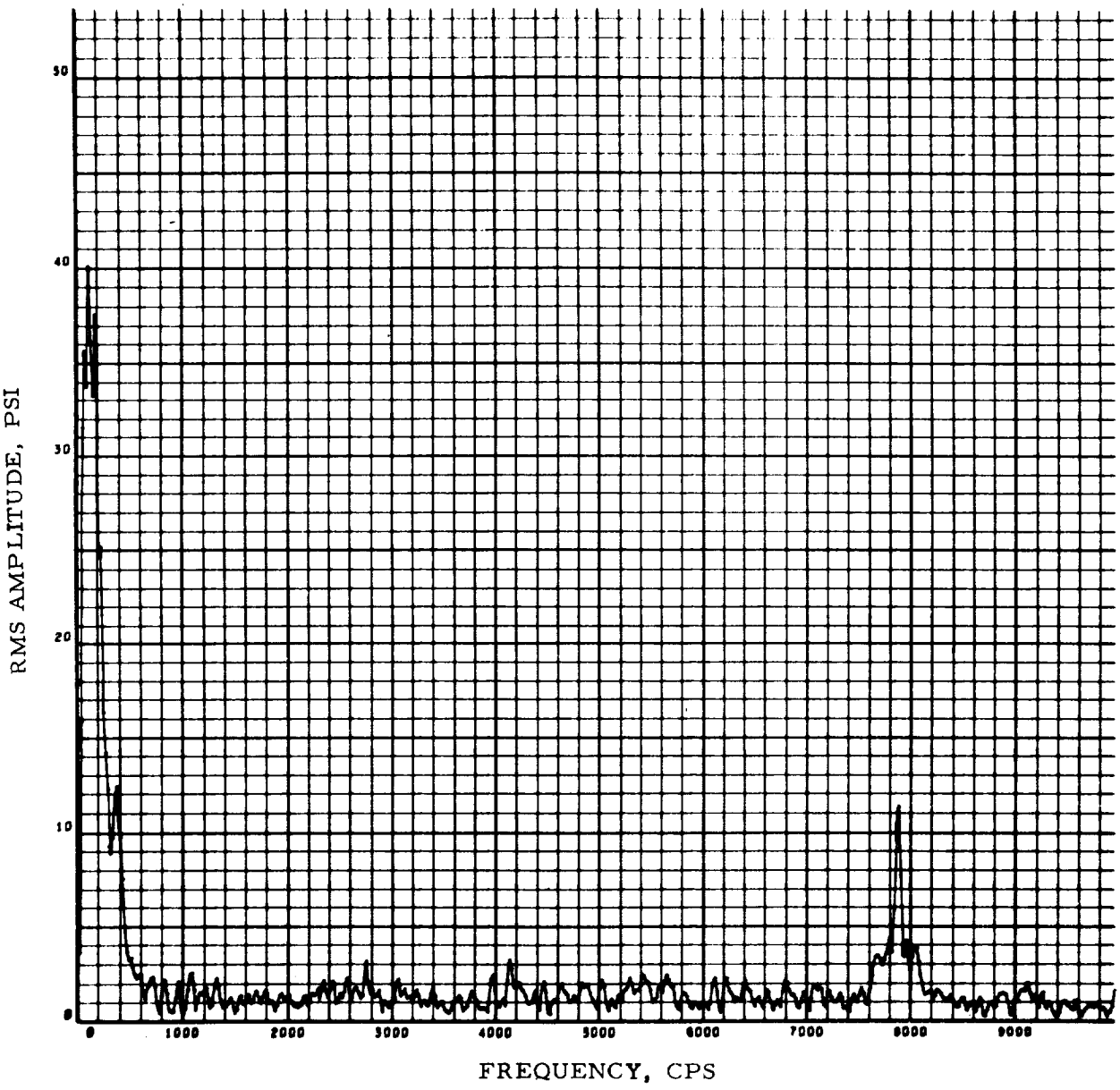

FIGURE 10. FREQUENCY ANALYSIS, RUN 147-25, FIRST TIME SLICE

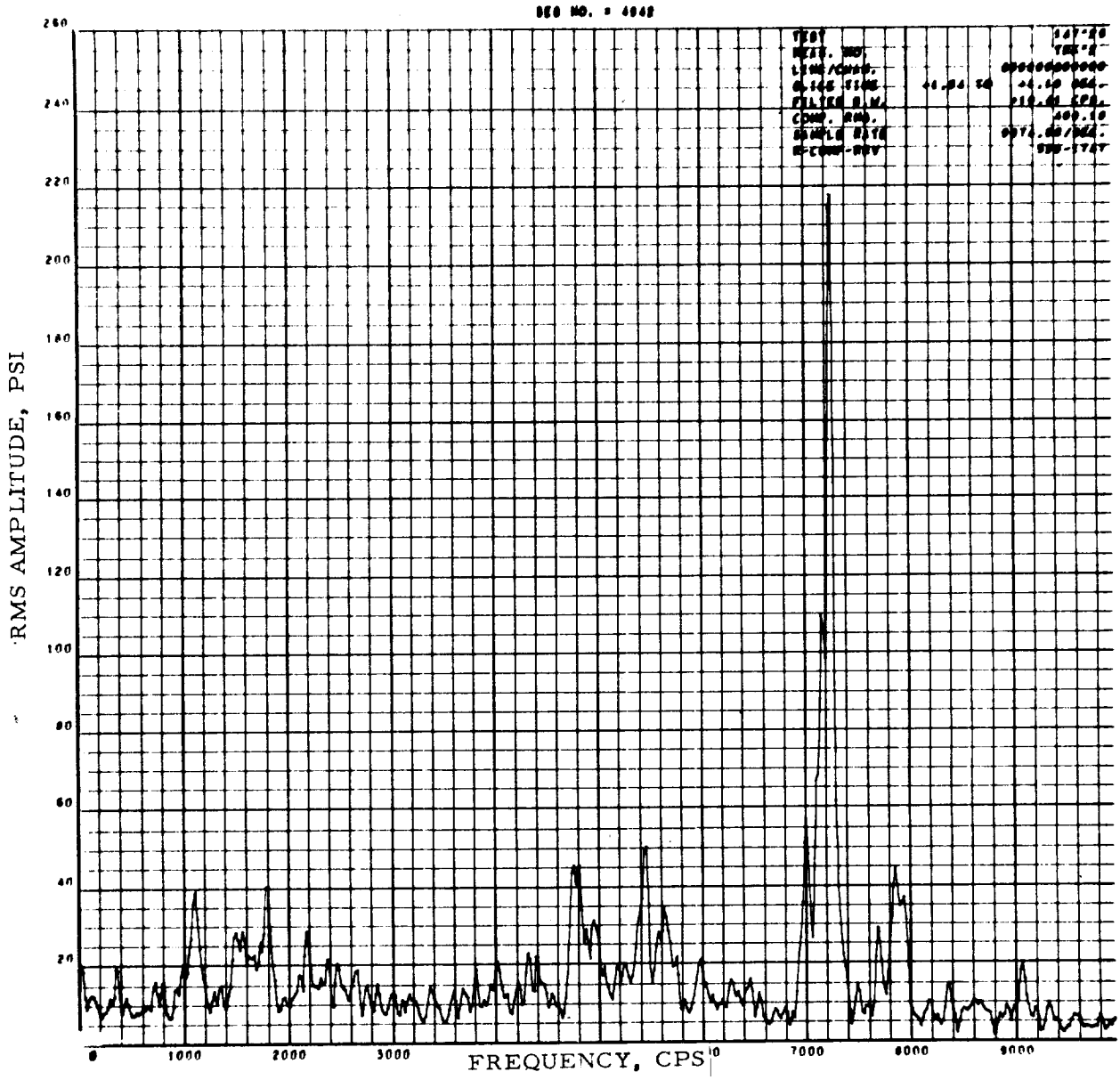

FIGURE 11. FREQUENCY ANALYSIS, PRESSURE NO. 3, RUN 147-25, SECOND TIME SLICE

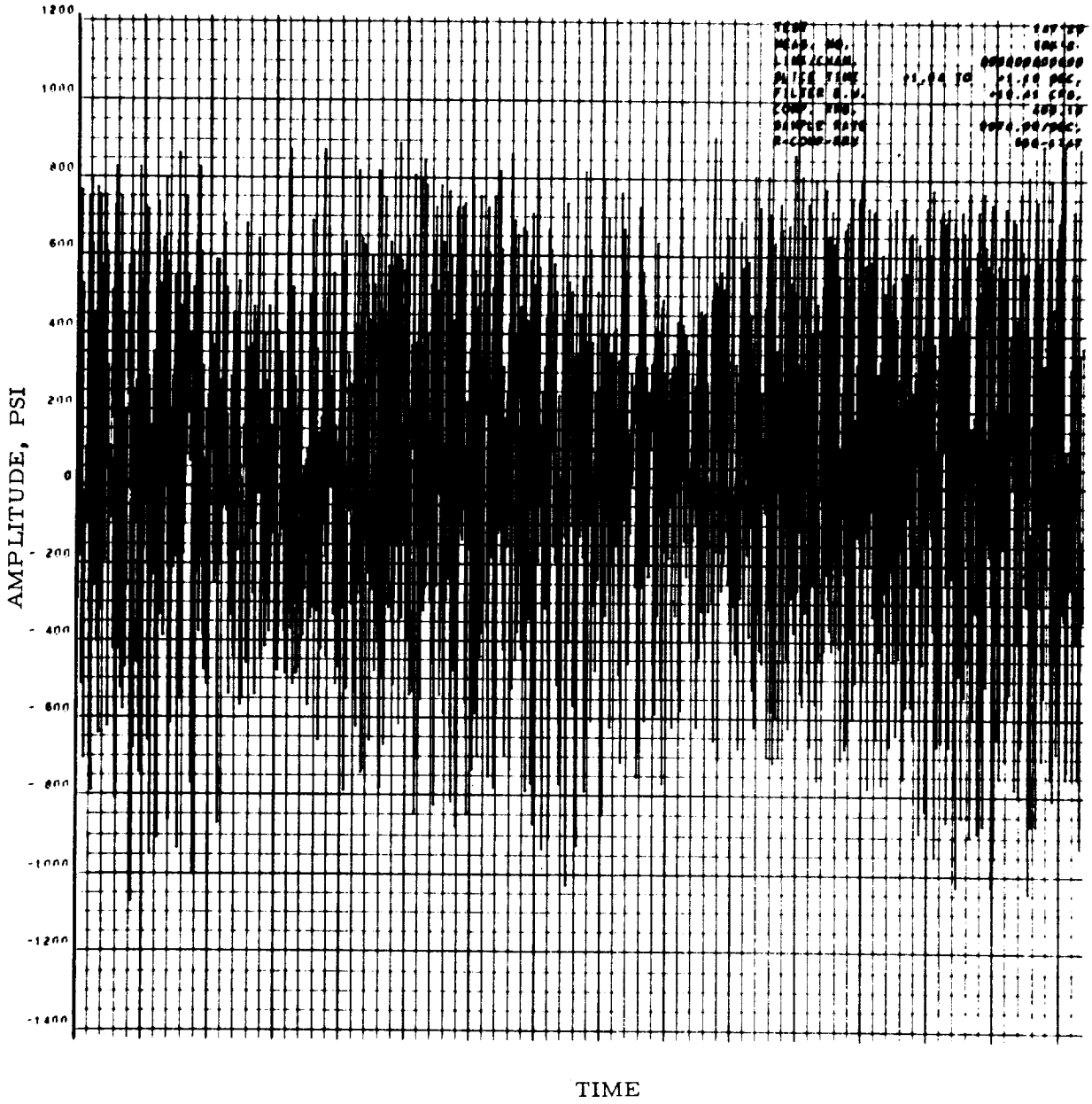

FIGURE 12. DIGITIZED INPUT DATA FOR FIGURE 11 PLOT

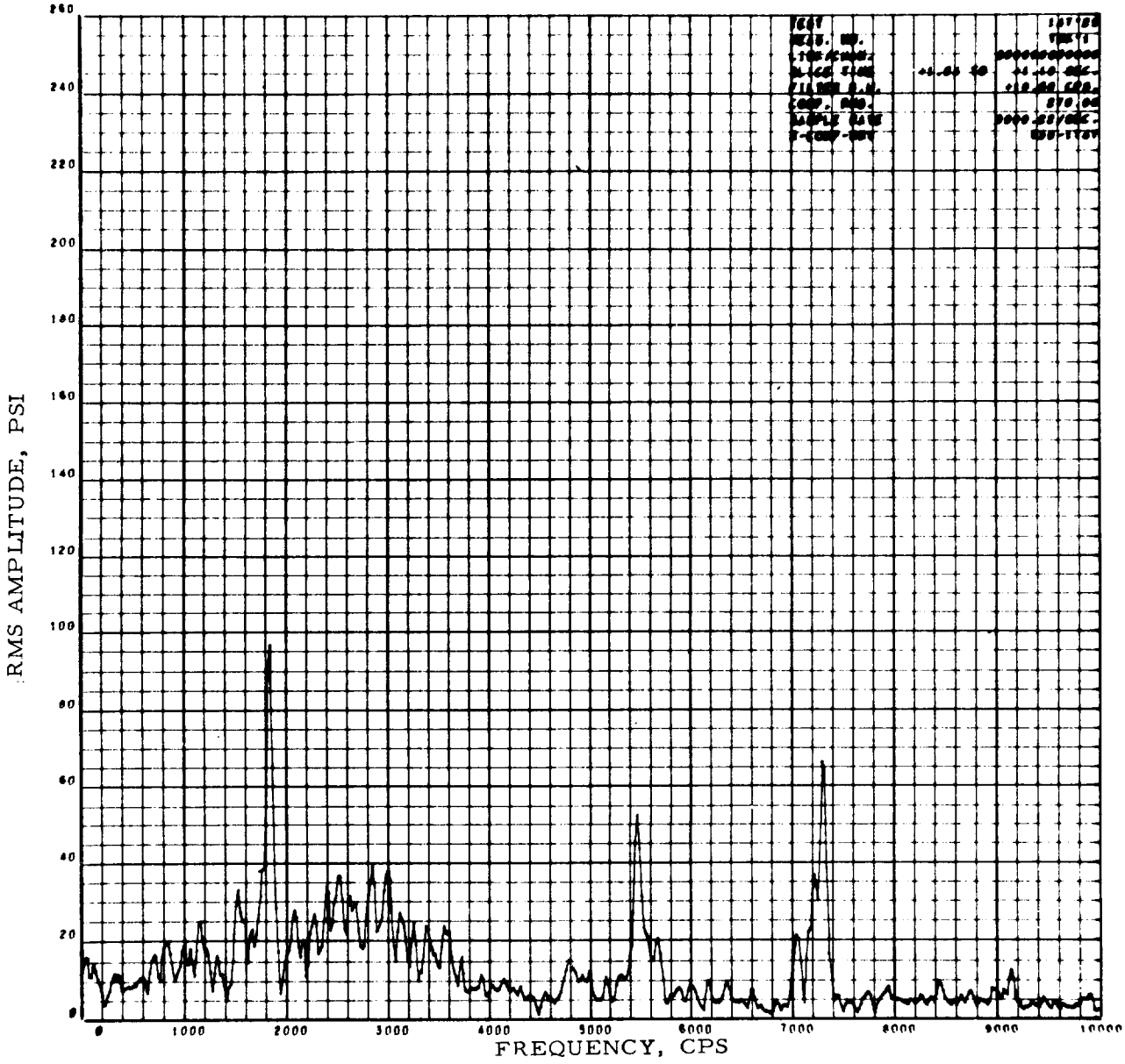

FIGURE 13. FREQUENCY ANALYSIS, PRESSURE NO. 2, RUN 147-25, SECOND TIME SLICE

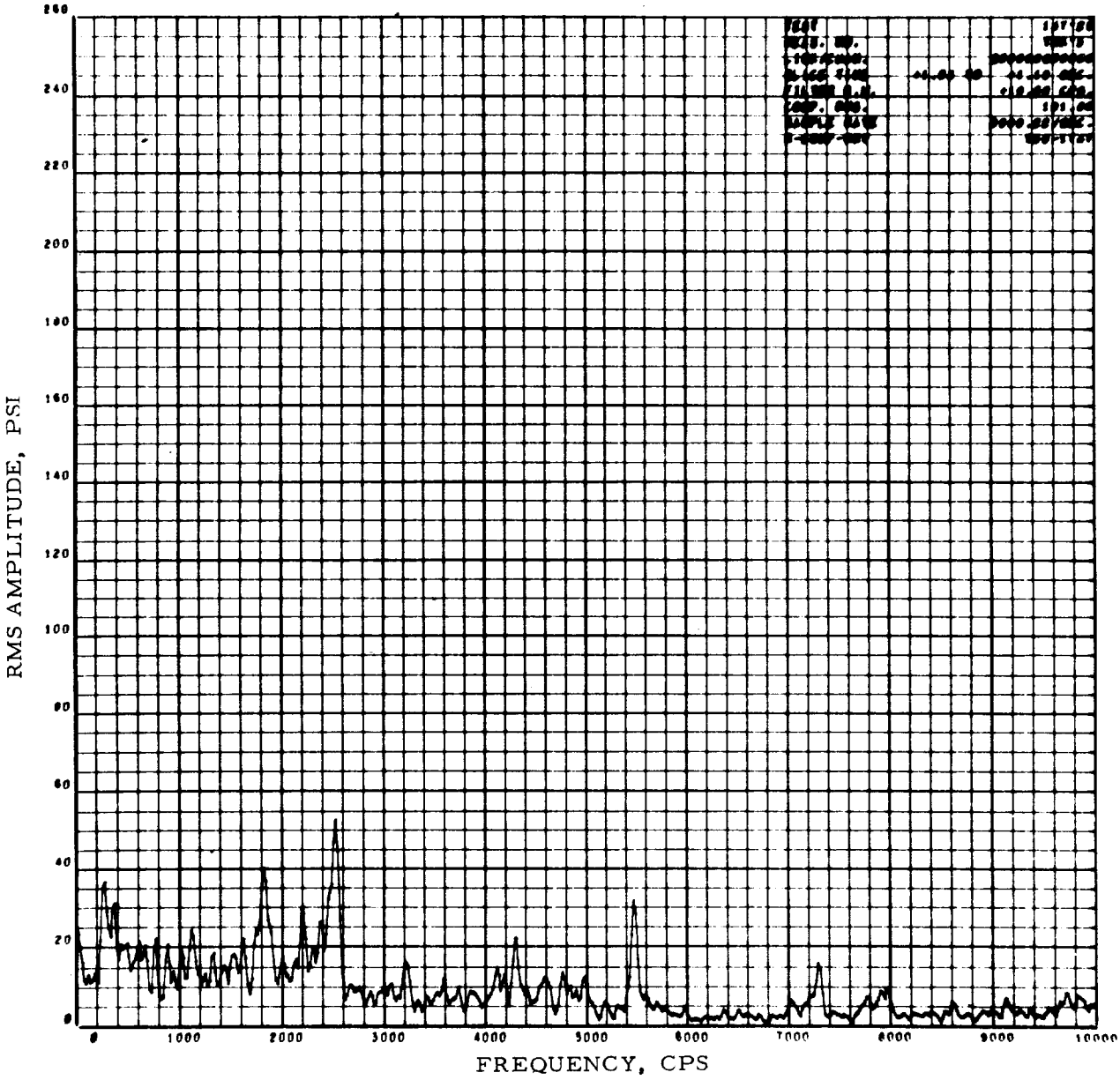

FIGURE 14
FREQUENCY ANALYSIS, PRESSURE NO. 4, RUN 147-25,
SECOND TIME SLICE

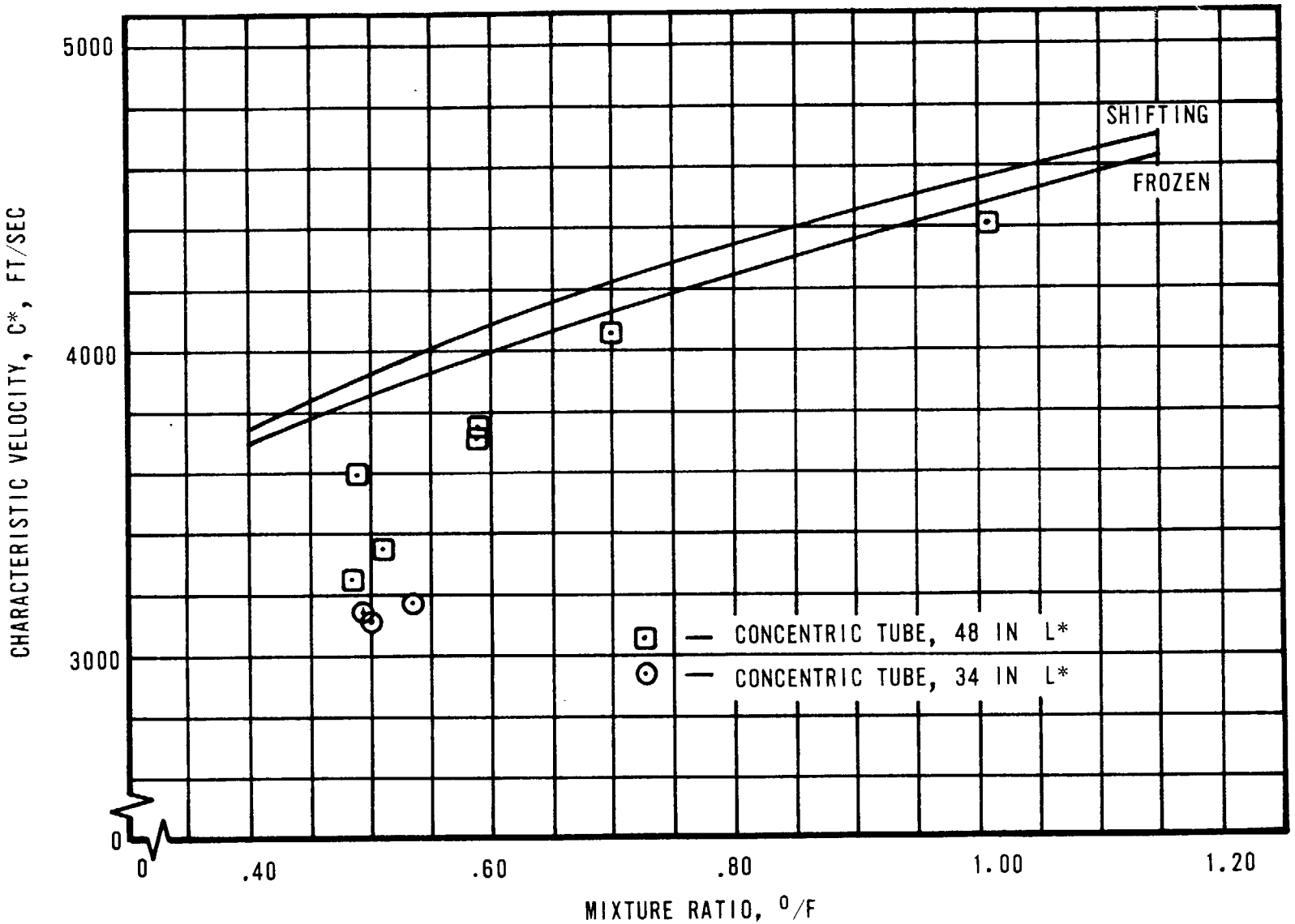

FIGURE 15
CHARACTERISTIC VELOCITY AS A FUNCTION OF MIXTURE RATIO,
M. R. = 0.4 TO 1.2

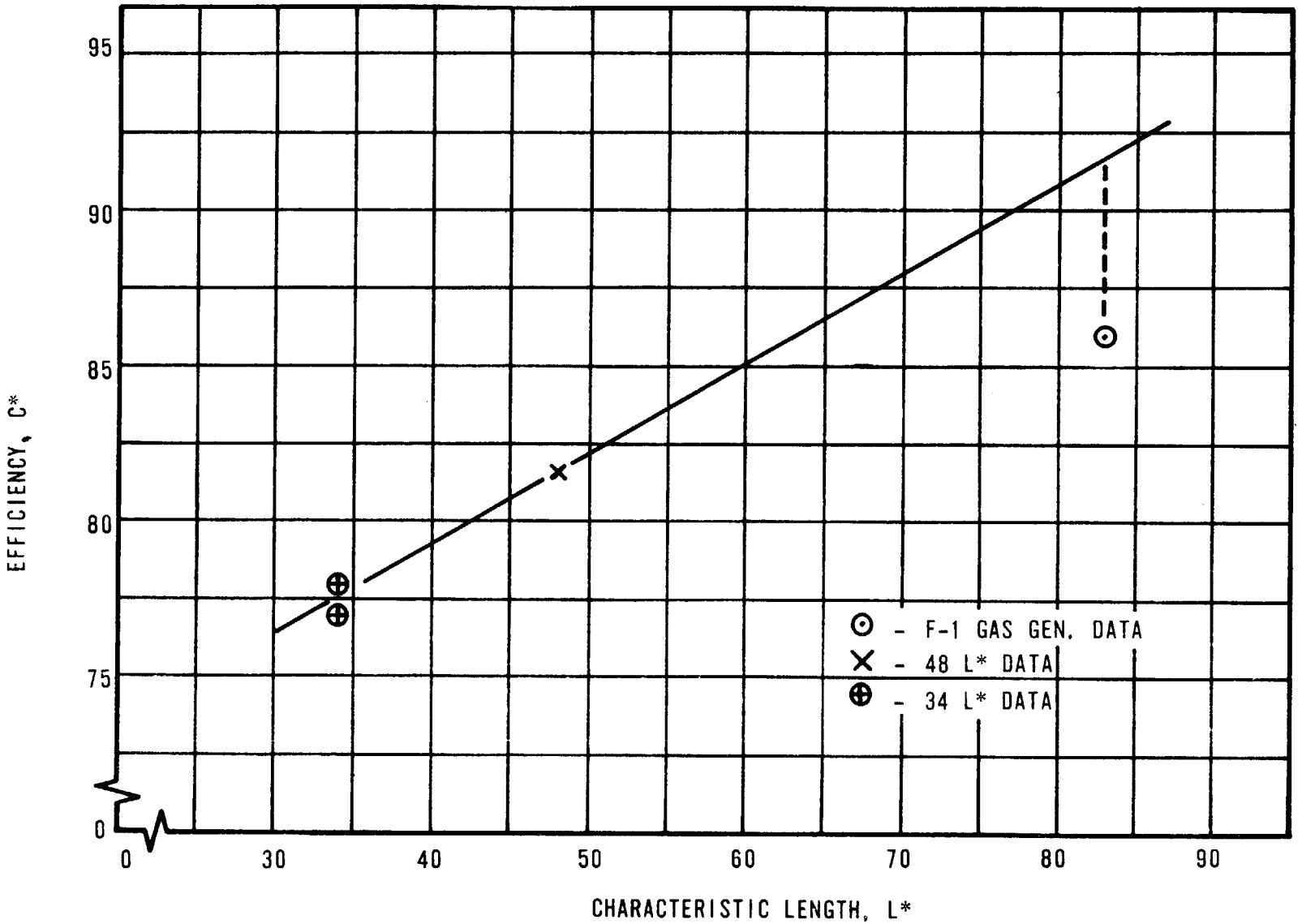

FIGURE 16
CHARACTERISTIC VELOCITY EFFICIENCY AS A FUNCTION
OF CHARACTERISTIC CHAMBER LENGTH, M. R. = . 48

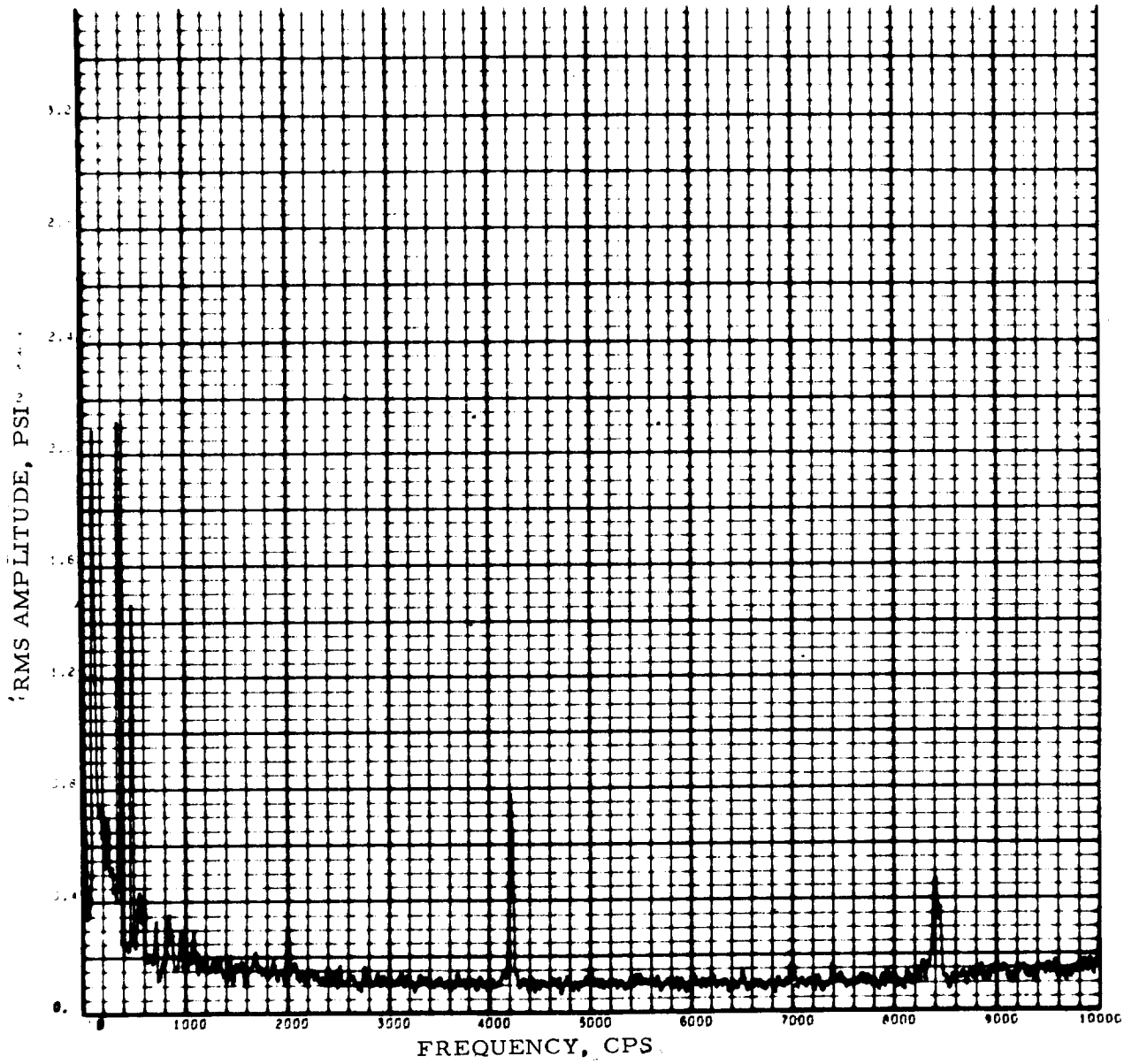

FIGURE 17
FREQUENCY ANALYSIS, PRESSURE NO. 3, RUN 147-21

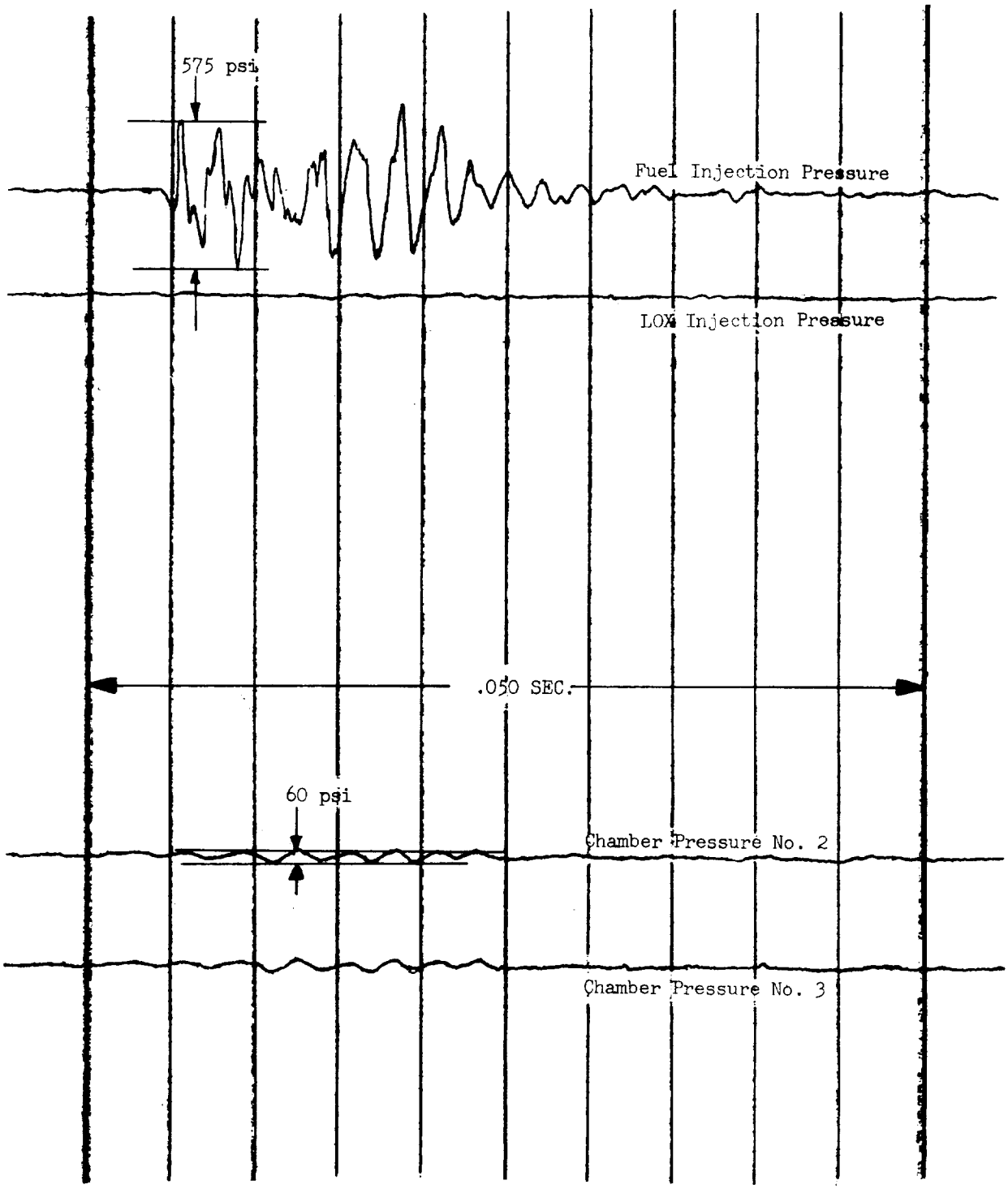

FIGURE 18
TRANSIENT PRESSURES RESULTING FROM FUEL LINE
PNEUMATIC PULSE, RUN 147-21

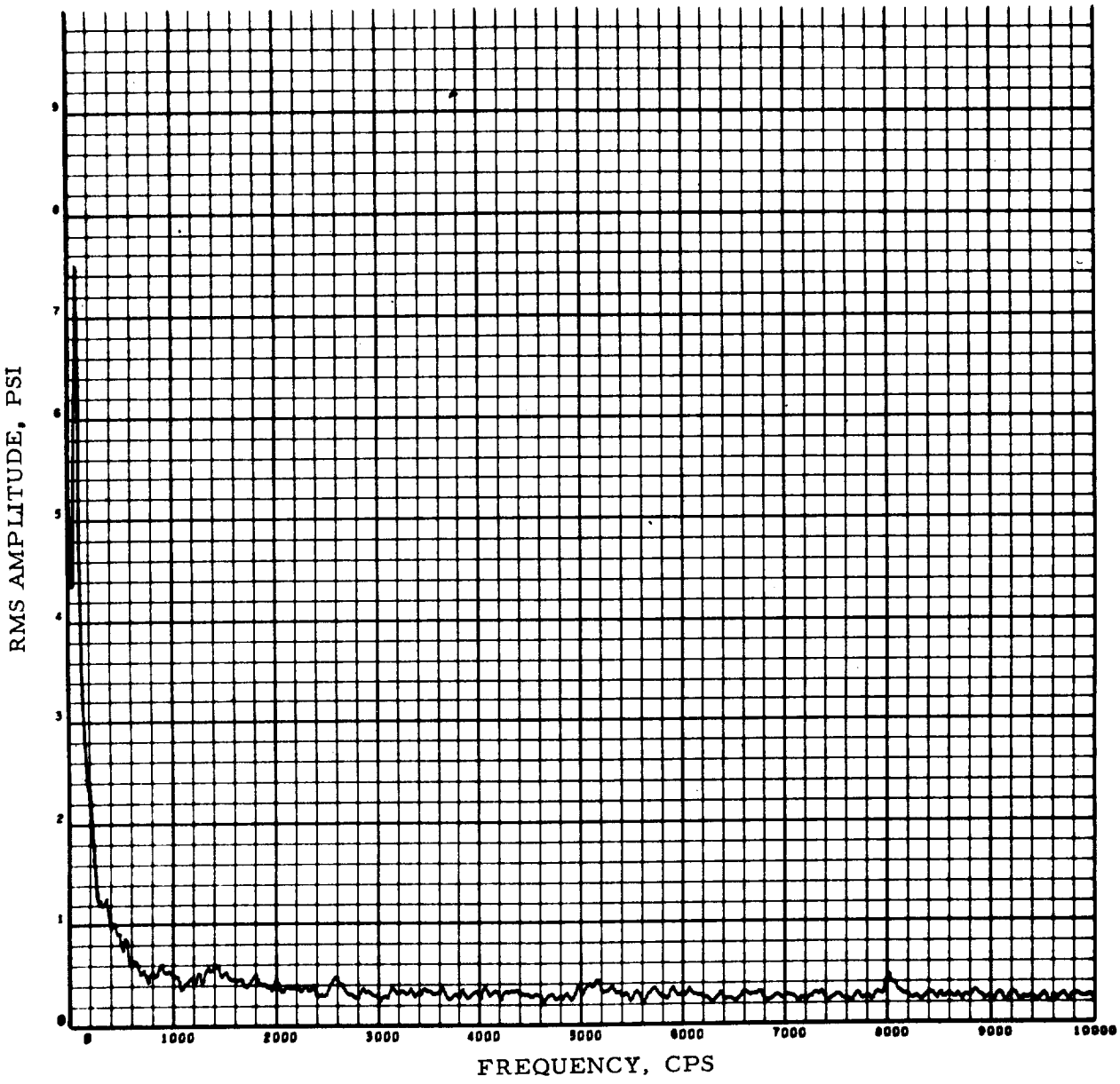

FIGURE 19
FREQUENCY ANALYSIS, PRESSURE NO. 2, RUN 147-19

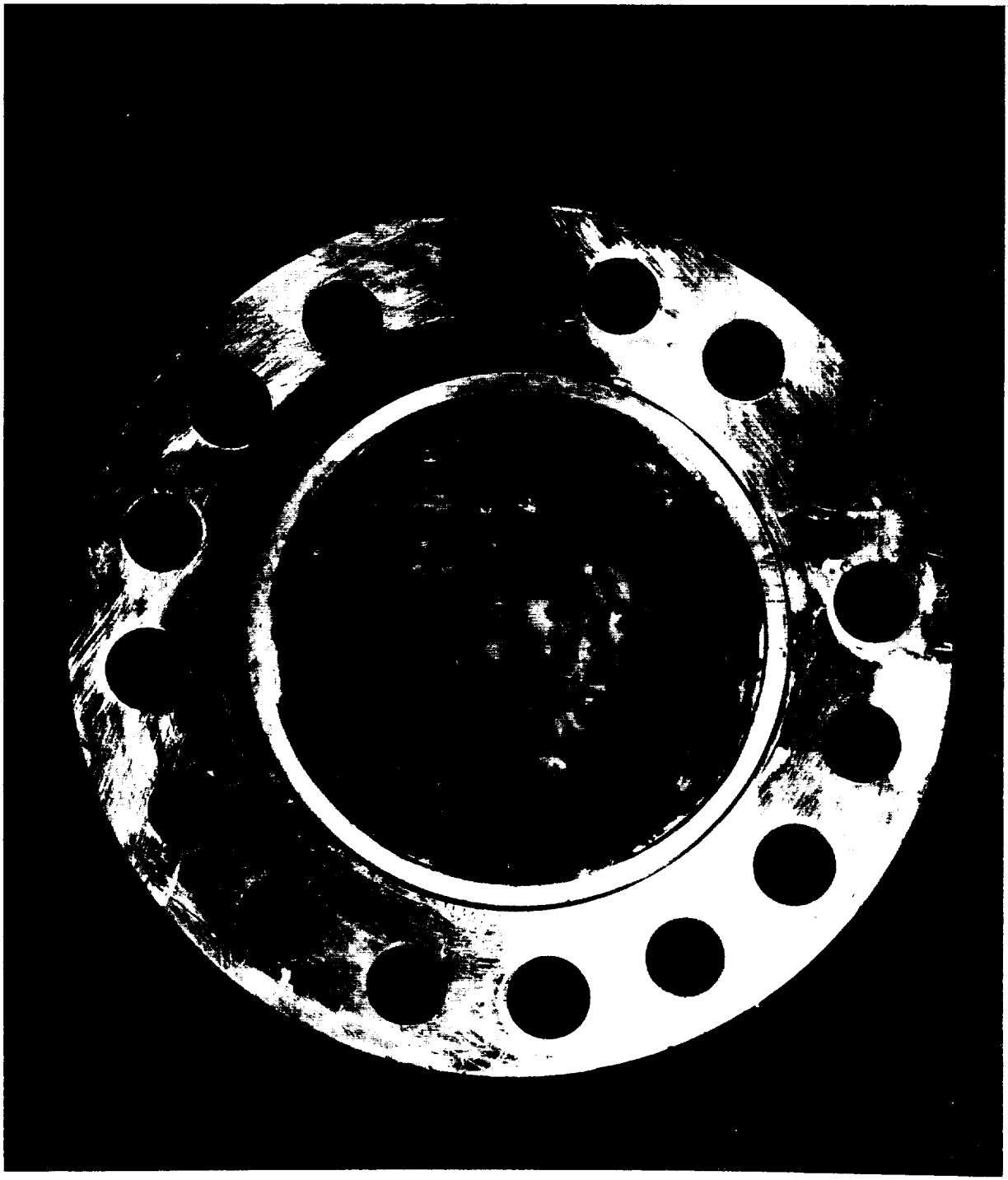

FIGURE 20. FACE HEATING PATTERN OF IMPINGING JET INJECTOR

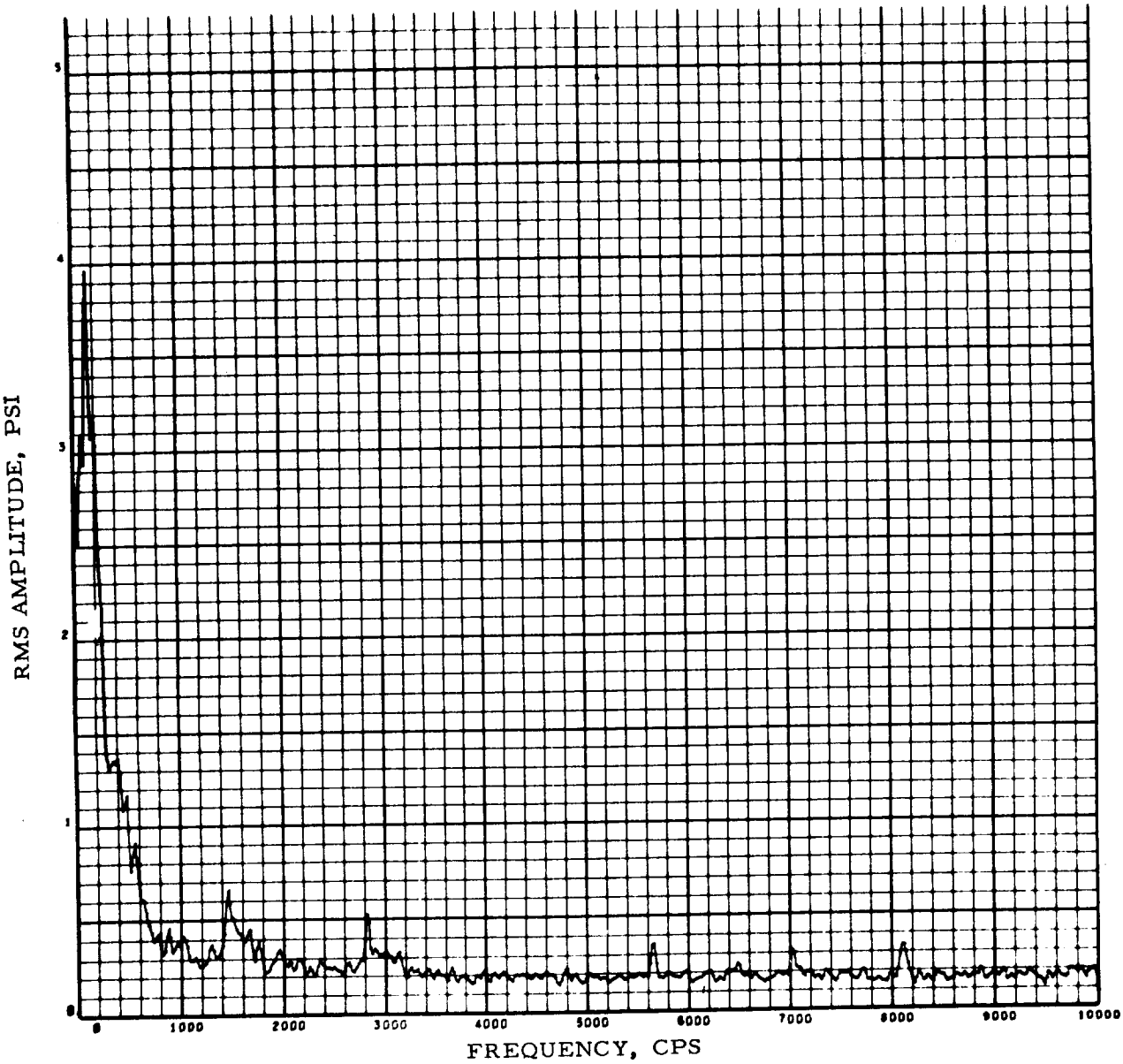

FIGURE 21
FREQUENCY ANALYSIS, PRESSURE NO. 3, RUN 147-31